

## Characteristics of night-time absorption spike events

A. Aminaei<sup>1</sup>, F. Honary<sup>1</sup>, A. J. Kavanagh<sup>1</sup>, E. Spanswick<sup>2</sup>, and A. Viljanen<sup>3</sup>

<sup>1</sup>Department of Communications Systems, Lancaster University, Lancaster, UK

<sup>2</sup>Department of Physics and Astronomy, University of Calgary, Calgary, Canada

<sup>3</sup>Space Research Unit, Finnish Meteorological Institute, Helsinki, Finland

Received: 7 October 2005 – Revised: 24 February 2006 – Accepted: 6 June 2006 – Published: 9 August 2006

**Abstract.** Sudden increases in cosmic radio noise absorption, known as spike events, have been identified as signatures of substorms in the previous studies. Using data from the IRIS (Imaging Riometer for Ionospheric Studies) at Kilpisjärvi, Finland ( $L \sim 6$ ) more than 450 night-time spike events between 1994 and 2003 have been identified. Spike events fall into four distinct categories based on their structure and the background magnetic activity as indicated by a local westward electrojet (IL index) derived from the IMAGE (International Monitor for Auroral Geomagnetic Effects) magnetometer network as well as Pi2 magnetic pulsations from SAMNET (The UK Sub-Auroral Magnetometer Network). Classifying the types of absorption spikes allows for identification of phenomena such as multiple onsets and pseudobreakups from riometer data. In addition we have studied the statistical variation of absorption spikes and their sub-classes. This includes examining the magnetic local time (MLT) distribution and the seasonal and solar-cycle variation in spike occurrence.

Those that seem to represent substorm onsets show a decidedly different MLT variation to those isolated spikes that represent pseudobreakups. The occurrence of spikes during different levels of geomagnetic activity is examined using the  $K_p$  index.

Wavelet analysis has been used for studying the temporal structure of spikes; also the direction of motion of spike events and localisation of spikes are presented for all events and each sub-class and results are compared with previous studies.

Statistical studies are supported with X-ray images of aurora from PIXIE (The Polar Ionospheric X-ray Imaging Experiment) when available.

**Keywords.** Magnetospheric Physics (Auroral phenomena; Energetic particles, precipitating; Storms and substorms)

Correspondence to: A. Aminaei  
(a.aminai@lancaster.ac.uk)

### 1 Introduction

Absorption spike events have been studied since 1965 when they were first described as fast onsets or “F events” (Parthasarathy and Berkey, 1965). Night-time spike events, which seem to have a close link with substorm onsets (Hargreaves et al., 1997), have had their various properties identified and studied since then. The spike event is identified as a sudden high intensity increase in absorption followed by a rapid decrease within few minutes.

Originally they were thought to be east-west extended strips of precipitation moving through riometer beams (Hargreaves et al., 1979) with north-south extents of the order of tens of km (Nielsen and Axford, 1977). Nielsen (1980) assumed spikes were caused by enhancement in electron density at 90-km altitude.

Later studies have shown that spikes are actually elliptical regions of precipitation-induced ionisation, with typical dimension in the order of 170–190 km by 70–80 km.

Such an impulsive precipitation of electrons has been observed during spike events using balloon measurements of X-rays. They occurred near the onset of substorms and were accompanied by westwards or northwards movement of substorm surges (Bjordal et al., 1971). Later on, in a similar study, Pytte and Trefall (1972) observed magnetic Pi2 pulsations in the auroral zone magnetometers during the occurrence of impulsive precipitation and absorption spikes and concluded that events correspond to a transition from dipole-like field lines to significantly stretched field lines.

Spike events are very dynamic with speed in the range of a few 100 m/s to a few km/s (Hargreaves et al., 1997). The spikes, which were observed in both hemispheres, tend to move poleward and westward, though examples of eastward motion and cases of equatorward motion have also been found (Hargreaves et al., 2001).

Using the wavelet technique Hargreaves et al. (2001) analysed the structure of spikes during 5–10-min periods. For those having poleward motion they found significant modulation between 16–67 mHz. They also reported similar

periodicities for magnetic Pi pulsations at the corresponding time and location and suggested that spike events and substorm onsets have a common source in the thin current sheet of the magnetotail following observations by Holter et al. (1996). Besides substorms, pseudobreakups are another magnetic activation candidate to be associated with absorption spikes (Spanswick et al., 2005).

Previous studies of pseudobreakups have distinguished them from substorms via their characteristics such as short duration (less than 10 min) and small intensity (less than 100 nT) (e.g. McPherron, 1991). More recently Aikio et al. (1999) showed that there is no definitive quantitative distinction between the two; both occur with reconnection process and are associated with a substorm current wedge formation, mid latitude magnetic Pi2 pulsation and particle injection mechanisms. However, pseudobreakups are identified by their short-lived periods without significant poleward expansion. Aikio et al. (1999) also indicated that pseudobreakups could be observed as isolated events as well as accompanying substorms onsets.

A variety of spike events occur in the dayside ionosphere. These have been related to magnetic impulse events (MIEs) (Terkiltsen et al., 2001) and are generally of much weaker intensity, usually of the order of 0.2–0.3 dB with durations of 1–2 min (Stauning and Rosenberg, 1996).

For this study dayside spikes have been eliminated and only absorption spikes that occur between 15:00–24:00 UT ( $\sim$ 17:45–02:45 MLT) have been considered. These events include high and sudden variations of absorption data in the IRIS field of view (FoV). Magnetometer data as well as changes in local electrojet index (IL) have also been considered simultaneously to address any geomagnetic features related to the structure of absorption spike events.

## 2 Observations

Absorption spike events have been detected using data from the IRIS in Kilpisjärvi, Finland, centred at 69.05° N, 20.79° E, and L-shell  $\sim$ 6. IRIS measures auroral absorption (AA) via an array of 49 narrow-beams (widths between 11.2° and 13.9°), which produces a 2-D image of absorption in a large region of sky ( $\sim$ 220 km  $\times$  220 km at 90-km altitude). In addition, the Kilpisjärvi IRIS has a single widebeam riometer and operates at 38.2 MHz; IRIS samples cosmic noise absorption in every beam each second. AA is due to energetic particle (mostly electron) precipitation; high-energy electrons ( $>$ 10 keV) ionise the D and lower E region and cause AA. Since AA is dependent on the energy and flux of electron precipitation, sudden increases in energetic electron fluxes at energies in the range of tens of keV are associated with spike events (e.g. Pytte and Trefall, 1972).

Another important factor for producing night-time spike events is the mechanism of acceleration of energetic parti-

cles which happen during dipolarization of magnetic fields in substorm events. (e.g. Aggson et al., 1983).

In addition to riometer data, magnetometer data were obtained from the IMAGE station at Kilpisjärvi for events that occurred after 1998 when data were available. This is archived at high resolution (1-s) as part of SAMNET. All three components of the magnetic field measurements were examined during each event to observe variations and Pi2 pulsations during spike events. These components are H, horizontal magnetic northwards, D, horizontal magnetic eastwards, and Z, vertically downward components.

A local AL index (IL) was derived from IMAGE data and was employed to match up the spike events with local, larger scale magnetic variations potentially connected with substorm-like activity. The local AL (AU) index is constructed by taking the minimum (maximum) envelope of the northward components of the IMAGE magnetometer stations. The intensity of the index depends on the magnitude of the electrojets so that 1 nT changes of local indices roughly corresponds to 1000 A of electrojets. There are two main currents, which occur regularly in the auroral region; eastward (EEJ) and westward electrojet (WEJ). Since the northward magnetic field increases with EEJ and decreases with WEJ, EEJ and WEJ can be distinguished in ground stations by looking at local indices; besides the EEJ flows during the local evening whilst the WEJ is usually observed around local midnight. The IL index has been used to detect the substorm phases (e.g. Tanskanen, 2002) meanwhile the precise timing of substorm onsets is detected by Pi2 pulsation (e.g. Aikio et al., 1999).

When available, PIXIE images have been used to provide aurora observations during spike events. PIXIE is an X-ray camera aboard the Polar spacecraft. Images include fluxes up to  $1.6 \times 10^4$  photon/(cm<sup>2</sup>-sr-s) of X-rays (2–12 keV) generated by precipitating electrons with energy from a few keV to more than 30 keV, which determine the intensity of energetic precipitation when aurora occurs (Imhof et al., 1995).

### 2.1 Criteria for identification of spike events

IRIS widebeam data has been used in this study to detect spike events. Assuming that the spike events usually take no more than 5 min (Hargreaves et al., 2001) conditions were set to identify events in which widebeam data (using 2-min averages) rose from the level of noise/background absorption to more than 1-dB intensity then fell down to the level of noise/background absorption in three successive points. 450 events were selected from the period of September 1994 when IRIS became operational until March 2003. A minimum of 1 dB was set for spike detection in order to eliminate low intensity events since they might be mixed up with maximum intensity of AA patches. Absorption patches mainly move with  $\mathbf{E} \times \mathbf{B}$  drift of electrons therefore their velocity seems to be different from motion of spike events (Nielsen, 1980).

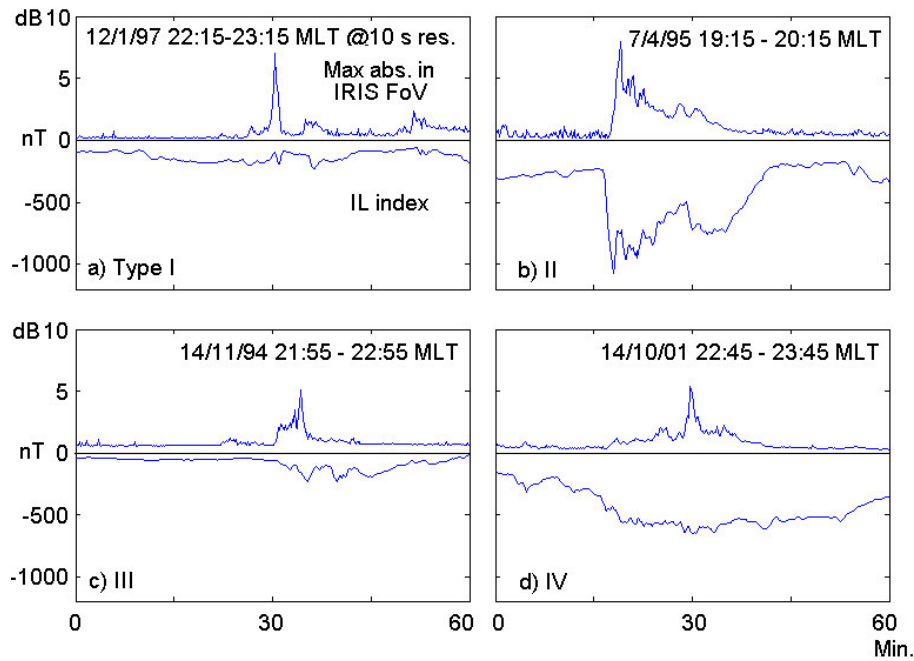


**Fig. 1.** Typical examples for 4 types of absorption spike events. Data are maximum absorption in IRIS field of view in dB and IL index in nT both at 10-s resolution and in 1-h interval.

One should note that night time spike events might not be observed for a couple of nights during quiet periods and there might be several per night in active conditions. IRIS samples cosmic noise absorption (CNA) every second, but for this study we have used 10-s averages. This matches the resolution of the IL index from the IMAGE chain. We used the maximum absorption observed over the whole imaging riometer array in our analysis in the same manner conducted by Hargreaves et al. (2001); following event identification, narrow-beam data were used to identify the direction of motion of spikes across the IRIS field of view.

Events were examined within 1-h intervals to identify absorption related to the precipitation of electrons, which had been recently injected into the inner magnetosphere from the magnetotail (e.g. Baker et al., 1981). Forthwith, this shall be referred to as injection absorption. Some examples contained multiple spikes within the 1-h interval. Considering spike events typically last few minutes 1-h duration seems to be long enough to find out possible relation between events and reconnection activations. It should be noted that although substorm events typically last more than one hour (e.g. Tanakanen, 2002) they are often a combination of many onsets and breakups (Aikio et al., 1999) and each onset and/or breakup may be accompanied by a spike event. Previous work by Hargreaves et al. (2001) was based on a short period (within a few minutes) analysis of selected spike events (these events are also among the 450 events we detected), and demonstrates the temporal properties of spikes. In this study we picked events occurring during 15:00–24:00 UT,

which covers roughly 6 h before and 3 hours after magnetic local midnight (MLM) at ~21:15 UT at Kilpisjärvi.

## 2.2 Classification of spike events

Absorption spikes have been classified by their structure and temporal position relative to injection absorption. The term “injection absorption” is used to describe the background absorption that appears along with absorption spikes. During the substorm process energetic particles are injected from the magnetotail into the inner magnetosphere and subsequently precipitate to the ionosphere, hence the injection absorption is the result of precipitation of freshly injected electrons.

Four basic classes of spikes are identified:

- Individual spikes (type I)
- Spikes followed by injection absorption (type II)
- Spikes preceded by injection absorption (type III)
- Spikes embedded in injection absorption (type IV)

Figure 1a shows a typical type I spike accompanied with the variation in the IL index. Type I have negligible injection absorption. These spikes appear as a sudden increase of absorption which falls off rapidly after they reach their peak. Thus the temporal structure of type I spikes is almost symmetrical around the peak; the rise and decay time of spikes are of the order of a few hundred seconds.

Variations in the IL index are short and sharp as well. The recovery time of the IL index is the same as those of spikes.

**Table 1.** Number of events and the range and mean of maximum absorption in each type of spikes.

Type of spike events	No. of events	Range of max. absorption (dB)	Mean of maximum absorption (dB)
<b>I</b>	87	2.2–12.3	5.1
<b>II</b>	157	1.4–14.9	4.6
<b>III</b>	27	2.2–8.3	4.3
<b>IV</b>	204	1.6–12.6	3.9

Panel (b) in Fig. 1 shows a typical spike II event with IL index. These are similar to type I in that they start with a rapid increase of absorption and reach their peak shortly afterwards. However, the decay time of type II spikes is longer than their rising time, in the range of a few minutes to tens of minutes. The background absorption in this type decays (usually exponentially) from the peak of spike or some point lower to the zero level and might include smaller secondary spikes. The IL index in type II events starts with a sharp decrease from the zero level (order of minutes) to a local minimum followed by a more gradual recovery. The start of IL decrease occurs once spikes rise but the recovery time may take longer than the decay time of spikes.

Figure 1c shows a typical type III spike event; these start with injection absorption followed by spikes. In most of the events the IL index decreases gradually once injection absorption begins and it drops with a sharp slope once the absorption spike occurs.

A typical event of type IV with the corresponding IL variation is shown in Fig. 1d. Here, one or multiple spikes are embedded in a period of injection absorption. The difference between type IV and type III is that in type IV injection absorption is also observed after the spike. The corresponding IL index varies rapidly once a spike is observed. Type IV spikes have the longest duration of the order of tens of minutes. These events can also be considered to be combinations of types II and III.

### 3 Statistical analysis

Following the criteria stated in the preceding section 87 type I spike events have been identified. The maximum absorption varied between 2.2 and 12.3 dB with the mean of 5.1 dB and standard deviation (SD) of 2.29. 12% of type I spikes were followed by another spike event. 157 events of type II were found, peaking between 1.4 and 14.9 dB (mean=4.6 dB and SD of 2.11). For more than 40% of these events the recovery time of the IL index was longer than the decay time of the absorption spike. 27 events have been identified as type III with maximum intensity varying between 2.2 and 8.3 dB (mean=4.3 dB and SD of 1.66). More than

50% of type III spike events occurred with a gradually decreasing IL index following by absorption injection.

For type IV spikes 204 events have been identified, with the maximum intensity between 1.6 and 12.6 dB and the mean of 3.9 dB and SD of 1.59. Summary of statistics is shown in Table 1. Type I has, on average, the most intense spikes with shortest period of the order of a few minutes and type IV has, on average, the least absorption intensity with the longest duration, in the order of tens of minutes.

In the following sections daily, seasonal and yearly variations of spikes as well as their dependency on the  $K_p$  index are presented.

#### 3.1 Magnetic Local Time (MLT) dependency of spike events

Figure 2a shows the occurrence of spike events between 15:00 and 24:00 UT (17:45–02:45 MLT); Magnetic local midnight (MLM) is at  $\sim 21:15$  UT at Kilpisjärvi (69.05° N, 20.79° E,  $L \sim 6$ ). Pre-midnight events dominated, peaking 1–2 h before MLM. The median of the distribution is at 20:15 UT (23:00 MLT). Taylor (1986) reported similar results for spike events at Abisko (68.40° N 18.90° E,  $L=5.81$ ,  $MLM=21:30$  UT) during 1980–1985 with the distribution median at 20:25 UT (22:55 MLT).

According to Taylor's observations only a few events happened after 24:00 UT (02:30 MLT). Similar to the distribution of spike events, the occurrence of substorms has been reported as asymmetrical around MLM with pre-midnight substorm events dominating (e.g. Gérard et al., 2004).

High absorption events which occur after 24:00 UT (02:45 MLT) seem to fit in the morning sector absorption events rather than substorm related night-time spike events as our preliminary statistics show that these events have different structures with longer durations and lower intensities and sometimes with no corresponding variations of the magnetic components.

Figure 2b shows the distribution of each separate type of spike in MLT. For type I events the distribution is skewed strongly (43%) towards 19:00–21:00 UT (21:45–23:45 MLT) with a further 30% falling between 21:00–23:00 UT (23:45–01:45 MLT).

Only 2% of events occurred in the hour before 24:00 UT (02:45 MLT). Half of type II events occurred between 19:00 UT and 21:00 UT (21:45–23:45 MLT) with more even numbers around this time span. There were few type III events (27) with all but one occurring between 16:00 and 23:00 UT (18:45–01:45 MLT) in which 4% of events occurred between 16:00–17:00 UT (18:45–19:45 MLT). Type IV events occurred mostly later at night with the percentage of occurrence during 21:00–24:00 UT (23:45–02:45 MLT) reaching 44%.

As well as the occurrence of spikes in magnetic local time it is also worth examining the strength of those spikes in an

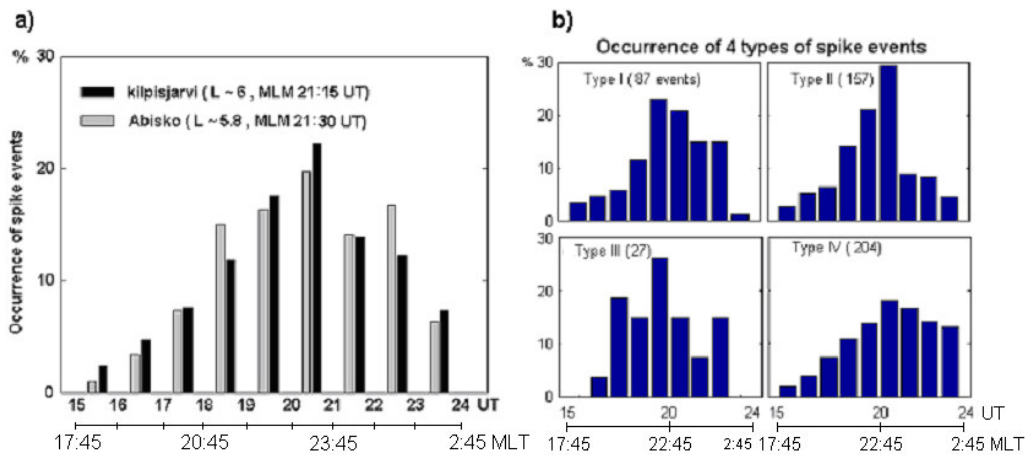


**Fig. 2.** (a) Occurrence of spike events between 17:45-02:45 MLT (15:00–24:00 UT). Black bars are data from IRIS at Kilpisjärvi (L~6.1, Magnetic Local Midnight ~21:15 UT) during 1994–2003. Data in grey bars are study done by Taylor (1986) representing the occurrence of spikes in Abisko (L~5.8, MLM 21:30 UT) during 1980–1985. (b) Occurrence of 4 types of spikes in the IRIS FoV between 17:45–02:45 MLT (15:00–24:00 UT) during 1994–2003.

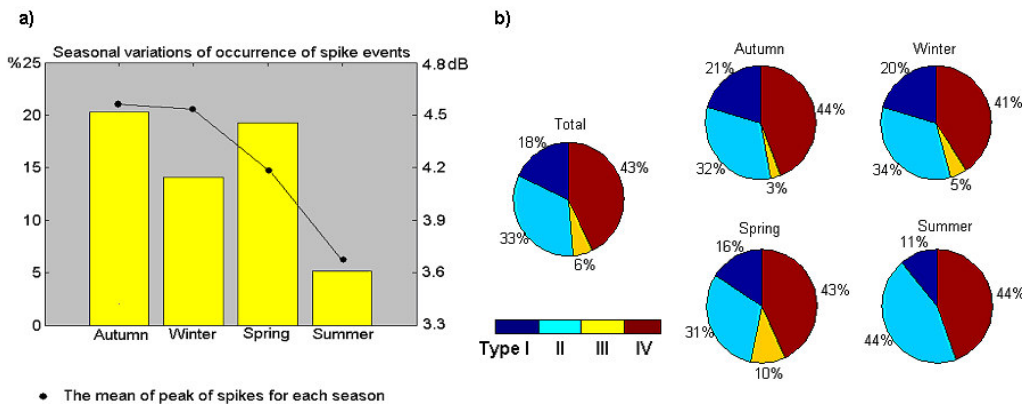


**Fig. 3.** (a) Seasonal variations of spike events in the IRIS FoV during 1994–2003. Bars are seasonal occurrence (event/day) of spike events and dots are the mean intensity of spikes for each season. (b) Total (left) and seasonal distribution of 4 types of spike events during 1994–2003.

attempt to determine whether there is a local time dependence on the level of precipitation that causes spikes.

A quarter of events have peak between 5 and 15 dB, though the majority of events (66%) vary between 2.5 and 5 dB. The variation of peak intensity for each event versus time illustrates that early evening events occurred less often but their intensities are slightly higher than the post midnight events. Both high and low intensity events were observed around magnetic midnight and most events occurred during 19:00–22:00 UT (21:45–00:45 MLT) with intensities varying largely between 2 and 12 dB.

One should note whilst afternoon-evening has the highest occurrence of huge spike events this period has been identified as time of minimum mean AA by previous statistical studies (e.g. Kavanagh et al., 2004). This minimum in diurnal absorption is thought to be caused by a reduction in wave

particle interactions during the afternoon sector of the magnetosphere (Kennel and Petschek, 1966). The average of AA then seems not to be affected by localised absorption spikes, which last for only a few minutes.

### 3.2 Seasonal and yearly variations of spike events

Seasonal variations of spike events are illustrated in Fig. 3a. The number of events has been normalised to the number of days when data were available. Seasons in this study are defined as symmetrical around one of the equinoxes or one of the solstices. Such seasonal periods have been used by Chua et al. (2004) for studying the seasonal variation of auroral substorms.

The occurrence (events per day) of spike events maximised during equinoxes with 20% and was minimum during

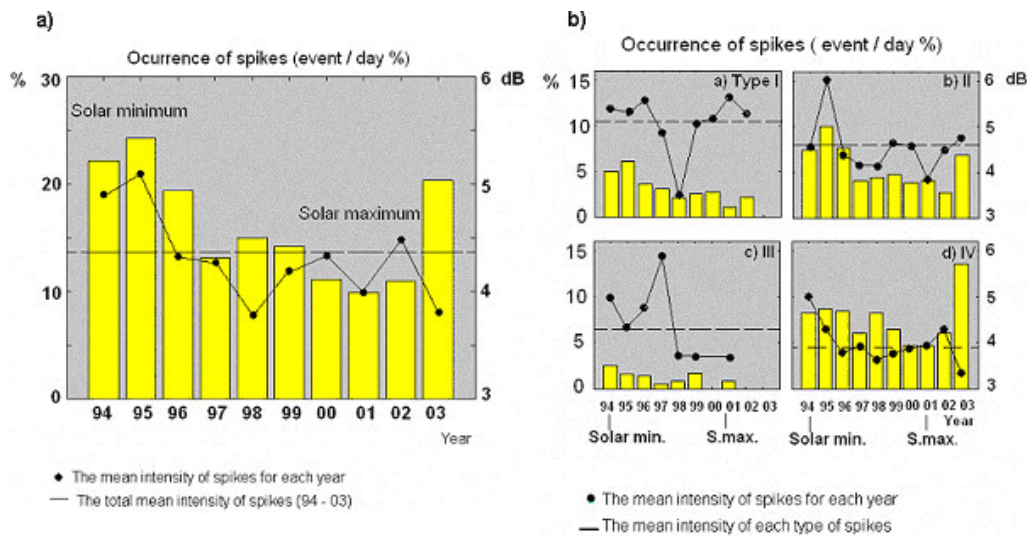


**Fig. 4.** (a) Yearly variations of spike events in the IRIS FoV during 1994–2003. Bars are yearly occurrence (event/day) of spike events and dots are the mean intensity of spikes for each year. Dashed line (---) is the mean intensity of all spike events (4.4 dB). Year 1994 is start of solar minimum and year 2001 is solar maximum. (b) Yearly variations for each type of spike events during 1994–2003. Dashed lines (---) are the mean intensity of each type of spikes.

summer (7 May–6 August) with 5%; the results are consistent with the seasonal variation of the occurrence of substorms (Hiebert et al., 2004).

The mean intensity of spike events was maximum during autumn (7 August–5 November) and winter (6 November–4 February) at  $\sim 4.5$  dB and it was minimum during summer (7 May–6 August) at 3.6 dB. Chua et al. (2004) found similar results for auroral breakups where they tend to be more intense and longer lived during dark hemisphere than those observed in the sunlit hemisphere and concluded that more energy is deposited by electron precipitation in the dark hemisphere during a substorm.

The seasonal variation can be due to the variation of angle between the Earth's axis and magnetotail, which affects the conditions for electron precipitation. Another possible explanation is that in the absence of sunlit ionosphere, density depletions lead to increased acceleration processes as described by Hamrin et al. (2005) when considering seasonal variation of discrete aurora. This indicates that the source of spike events is the enhanced flux of electrons of a few to 10-s of keV as opposed to 100s of keV.

Figure 3b demonstrates the occurrence of each type of spike as well as seasonal variation of each type of spike. While the occurrence of spikes has a similar pattern in autumn and winter, type III spikes were not observed during summer and had the maximum of occurrence during spring (10%). Type II spikes maximum occurrence was found to be in summer (44%).

The available (September 1994 to March 2003) data extends from the solar minimum of 1994 across the solar maximum of 2001. The median occurrence of events varies by

a little over an hour for individual years; from 19:48 UT (22:33 MLT) in 1995 to 20:53 UT (23:38 MLT) in 1996. Both 1995 and 1996 were active years with 76 and 69 events and median intensities of 4.11 and 4.03 dB, respectively. Year 2002 also had a high median intensity of 4.08 dB, but the number of events was much lower (49). The median and the mean absorption for all events were 3.76 dB and 4.36 dB (SD  $\sim 2$  dB), respectively.

Figure 4a shows that the number of events and the mean of absorption intensity were highest during the years closest to solar minimum (1994 and 1995), which is consistent with the past results of studying the occurrence of substorms (Hiebert et al., 2004).

This is possibly due to the tendency towards steady, high solar wind velocity which emanates from coronal holes during solar minimum; consequently the increased solar wind speed leads to enhanced coupling of the solar wind energy to the magnetosphere. Kavanagh et al. (2004) found similar results for the mean and median AA in which during 1995–2001 the IRIS absorption data maximised in 1995. Year 2001, which was the solar maximum, had the minimum occurrence of spikes with a low mean intensity of 4.0 dB.

Yearly variation of all types of spikes is shown in Fig. 4b. The peak of absorption intensity for type I was during the years 1996 and 2001. For type II 1995 had maximum intensity. For type III the peak was in 1997 and for type IV maximum was in 1994 and minimum in 2003. Years 1994 and 1995 had the maximum occurrence for types I, II and III. Minimum occurrence was in year 2001 for type I and III. For type II and IV minimum occurrence was in the years 2002 and 2000, respectively.

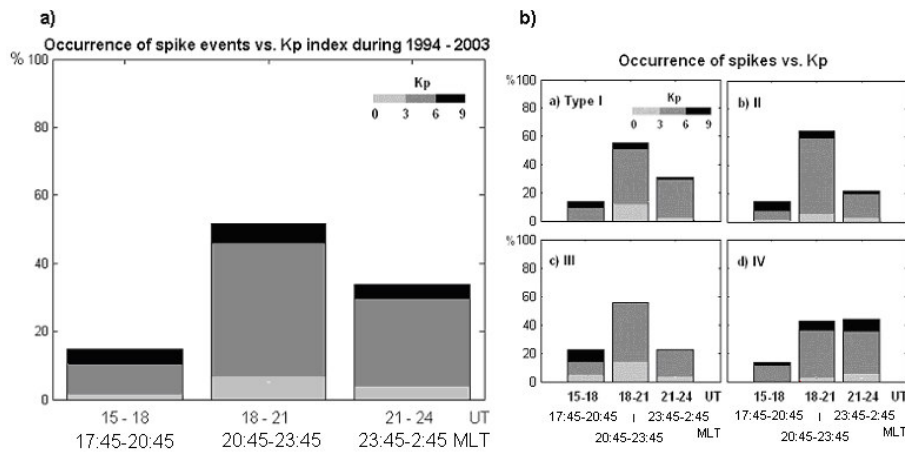


**Fig. 5.** (a) Dependence of spikes on the  $K_p$  index. Colorbars represent the occurrence of spikes during 3-hour time sectors versus 3 levels of  $K_p$  index. (light grey for events occurred during  $K_p$  smaller than 3, dark grey for events occurred during  $K_p$  between 3 and smaller than 6 and black for events occurred during  $K_p$  between 6 and 9). (b) Occurrence of 4 types of spikes versus  $K_p$  index is shown with similar colorbars.

### 3.3 Variations of spikes versus $K_p$ index

Kavanagh et al. (2004) demonstrated that the  $K_p$  index had the maximum effect on the mean of the AA from IRIS in the morning sector (~09:00 MLT) and minimal effect in the afternoon (~15:00 MLT). Here, a similar investigation has been carried out to examine what effect  $K_p$  index has on the variation of spike events.

Figure 5a shows all spike events binned by  $K_p$  index. More than 90% of spike events occurred during periods of  $K_p > 3$  and spike events in the periods of low  $K_p$  index ( $K_p \leq 3$ ) mostly occurred after 18:00 UT (20:45 MLT), which is consistent with the results of the study done by Nielsen (1980). Significant increases in the occurrence of spikes were observed when the  $K_p$  index increases from 0 to 3. For  $K_p \geq 4$  the relationship is not clear. In Fig. 5b the variation of each type of spike versus  $K_p$  index is illustrated. Type III events during low  $K_p$  are more numerous than the other types. Between 18:00 and 24:00 UT (20:45–02:45 MLT) there were more type IV spike events during high  $K_p$  ( $K_p > 6$ ). From 15:00 to 18:00 UT (17:45–20:45 MLT) the percentages of types II and III during high  $K_p$  are larger than those of type I and IV.

### 3.4 Relation of spike events to the magnetic Pi2 pulsations

Variations in magnetometer measurements have been examined for 220 events. In general the spike events were accompanied by a sudden decrease in intensity of the H component. For type IV spike events in which spikes were embedded in injection absorption, the H component decreased more slowly whilst the D component increased with approximately the same slope as the H component decreased. The Z component mostly decreased during spike events. Variations

in magnetic field intensity were of the order of a few hundred nano Teslas (nT) for all three components with no apparent linear relationship to the intensity of the spikes in dB. Several bipolar impulses appeared, mostly in the D and Z components following the onset of a spike. For multiple spike events sinusoidal oscillations were observed in the magnetic field components.

More details were yielded following an analysis of Pi2 pulsations in the magnetometer data. Pi2 pulsations are irregular geomagnetic field oscillations with periods between 40–150 s (Jacobs et al., 1964); these usually occur at substorm onsets so they are one of the more common signatures of substorms (Saito et al., 1976). Both magnetometers on spacecraft and ground stations, especially in the mid and low latitudes, detect Pi2 pulsations. This suggests they are a magnetospheric phenomenon since they exist both in the inner magnetosphere as well as the ionosphere (Baker et al., 1996). Hargreaves et al. (2001) analysed riometer data and detected Pi2 absorption pulsations as well as magnetic pulsations and compared the two.

We used the same filter (40–150 s) for magnetometer data as well as the IL index; the latter is used to identify the onset of substorms.

Pi2 pulsations were a common feature of all events. Magnetic pi2 pulsations usually occurred once absorption spikes peaked and then vanished as the absorption fell away. For sharp spikes (type I) they appeared in fewer cycles than those of spikes with injection absorption. The maximum peak-to-peak intensities mostly happened at or around spike onset and were around few tens of nT up to 125 nT. The time delay between two successive maximum peaks was of the order of 70–100 s corresponding to frequencies between 10–14 mHz which is consistent with previous ground and satellite-based studies of Pi2 pulsations (e.g. Keiling et al., 2001; Yeoman

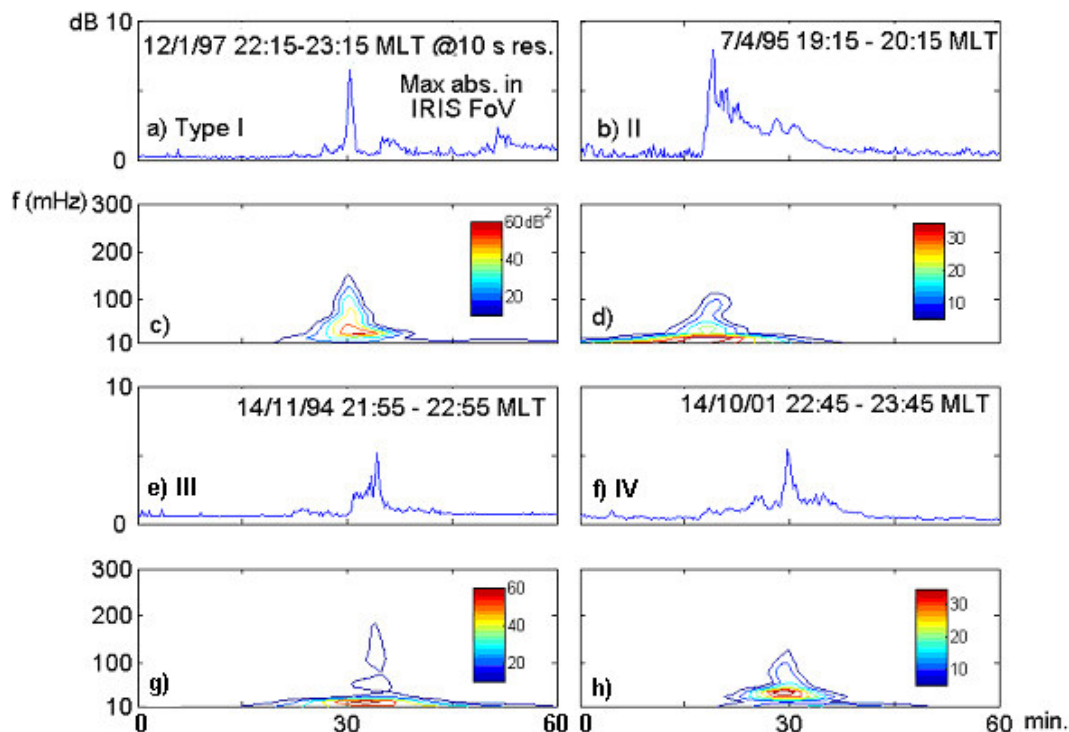


**Fig. 6.** Wavelet spectrum of 4 types of spike events. Panels (a), (b), (e) and (f) are maximum absorption in IRIS FoV in dB at 10-s resolution. Panels (c), (d), (g) and (h) are corresponding wavelet spectrum, respectively. Colorbar contours are in  $\text{dB}^2$  and the range of frequency is between 10 and 300 mHz. Data in all panels have 1-h period (x axis).

and Orr, 1989). Magnetic data from low latitude York station at  $L=2.57$  were also checked; the pi2 pulsations were similar to those at Kilpisjärvi ( $L=6$ ).

A Morlet wavelet was employed to study the structure of spike events both in the time and frequency domain across the hour containing each spike as opposed to the 5–10 min analysis carried out by Hargreaves et al. (2001). This longer period enabled the analysis of the structure of the whole absorption event including the spike itself and any accompanying absorption from absorption injection. The parameters of the wavelet function that was used are presented in Eq. (1):

$$\frac{1}{\sqrt{a}} \exp\left(\frac{jk(t-b)}{a}\right) \exp\left(-\left(\frac{t-b}{a}\right)^2\right). \quad (1)$$

Where  $k$ , a constant, equals 6,  $a$  is stepped over 30 values covering frequencies of 10 mHz to 300 mHz and  $b$  is the time shifting. The relevance of these terms is discussed in “a practical guide to wavelet analysis” (Torrence and Compo, 1998).

Results of analysis show that for most of the events the peak of the power spectrum lies in the frequencies up to 50 mHz but modulations of sharp spikes include higher frequencies up to 300 mHz. Hargreaves et al. (2001) found significant modulations in the frequencies between 16–67 mHz and 100–200 mHz. In our analysis no discontinuities were observed for those events having modulations up to 200 mHz and higher.

Figure 6 shows examples of wavelet spectra for 4 types of spike events. Maximum power spectrum in  $\text{dB}^2$  (red contours) for all types occurred in frequencies up to 50 mHz. For a better comparison, the maximum power for a range of frequency from 10 to 300 mHz (in 30 steps of 10 mHz) was derived. For each step the mean of the maximum power of each type of spike was normalised to the mean of the overall maximum power. Figure 7 shows the dimensionless results. In type I frequency components of power spectrum are nearly at the same level up to 40 mHz and they are reduced by 50% after 60 mHz (step 6). For type II and type III the frequency components are reduced by 50% after 40 mHz (step 4), while in type IV the frequency components drop quickly and they reduce by 50% in the second step (20 mHz). Results can be interpreted with structure of spikes in the time domain. Since type I has the narrowest structure in the time domain (shortest period) its spectra is expanded in the frequency domain. On the contrary type IV has the longest period in the time domain so its spectra is limited in the frequency domain.

### 3.5 Direction of motion of spike events

The motion of X-ray aurora has been considered using the 5-minute resolution PIXIE images during spike events. PIXIE images were available for 96 events in the period of 1996–November 2002. Most PIXIE images were obtained from

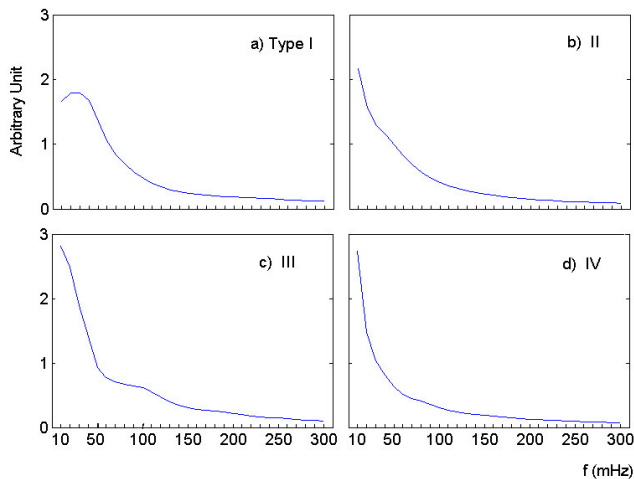


**Fig. 7.** Normalised mean of wavelet power spectrum for frequencies between 10–300 mHz (10 mHz step) for 4 types of spike events. Data bars are normalised to the mean of maximum power absorption and are dimensionless.

the apogee part of the Polar satellite's orbit and thus have a coarse resolution of typically 500–800 km.

For some events X-ray aurora emission was quite expanded covering a large area of the auroral zone and polar cap while in fewer events the X-rays aurora were localised. In 10% of events (10 out of 96 available events) the emission region expanded both westward and eastward. At least 16% of events had a poleward motion besides their west/eastward motions but only 5% of events recorded a southward motion.

Comparison of the maximum intensities of spikes with that of the X-ray emission showed no correlation, nor was there any major differences in the structure and development of the X-ray emission that occurred for different types of spike event.

We then followed the motion of spikes across the IRIS field of view. To determine the direction of spikes we picked up the beam in which the highest spike occurred for each event. We tracked its motion across the IRIS field of view both in north/southward and east/westward directions. The direction of spikes then yields using the position of the peak of spike in successive beams.

Figure 8 shows the motion of patch of absorption in IRIS FoV for the spike event occurred at 1 November 1995, 18:30–19:30 UT (21:15–22:15 MLT) in 10 s before the maximum absorption happened, at the time of the occurrence of maximum absorption and 10 s and 20 s later on, respectively. The motion of the patch of absorption is westward from panel (1) to (3) and it is north/westward from panel (3) to (4). As it can be seen the motion of patch of absorption is complicated in particular if longer period is concerned. Our studies confirm that the velocity of spikes are in the range of few hundreds meters per second to few kilometres per second as reported by Hargreaves et al. (1997). North/west ward mo-

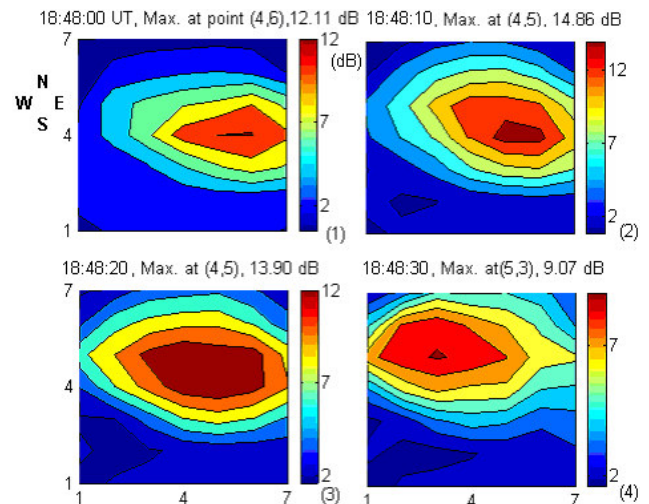


**Fig. 8.** Motion of patch of absorption in the IRIS FoV for spike event occurred in 1 November 1995, 18:30–19:30 UT (21:15–22:15 MLT) at 18:48:00, 18:48:10, 18:48:20, and 18:48:30 UT is illustrated in panels 1, 2, 3, and 4, respectively. Numbers in brackets determine the location of narrow-beams (vertically and horizontally) in which maximum absorption occurred. Colorbars are in dB. Geographic directions are indicated in the top left corner of figure.

tion of spikes in IRIS FoV was slightly dominated in type I. We could distinguish the motion of 51 events out of 87 events spikes for Type I. 45% of events had a northward motion while southward motion was observed for 25% of events. On the other hand westward events were 39% against eastward events of 31%. In type II the number of west/northward spikes was almost twice as east/southward spikes. No special direction was dominant for type III and IV spikes. The mean of maximum absorption (in dB) is slightly higher for west/northward spikes than those of east/southward spikes in all types of spikes.

### 3.6 Localisation of spikes

By considering both the IRIS FoV and the Sodankyla Geophysical Observatory (SGO) riometer chain it is possible to estimate the spatial coverage of spike events over a range of latitudes and a somewhat limited range of longitudes. It was found that for each type of spike observed by IRIS, corresponding spikes were also observed in the SGO chain. Figure 9 illustrates two successive spikes in the IRIS widebeam (red ovals). At the time that the first spike occurred at Kilpisjärvi (KIL, 69.05° N, 20.79° E), similar spikes were also observed at lower latitudes, down to Oulu (OUL, 65.05° N, 25.54° E). The second spike event was only observed at Kilpisjärvi and Ivalo (Iva, 68.55° N, 27.28° E). There is also a peak of absorption much further poleward at Hornsund; Svalbard (Hor, 77.00° N, 15.60° E) for the second event but its intensity is quite low. The

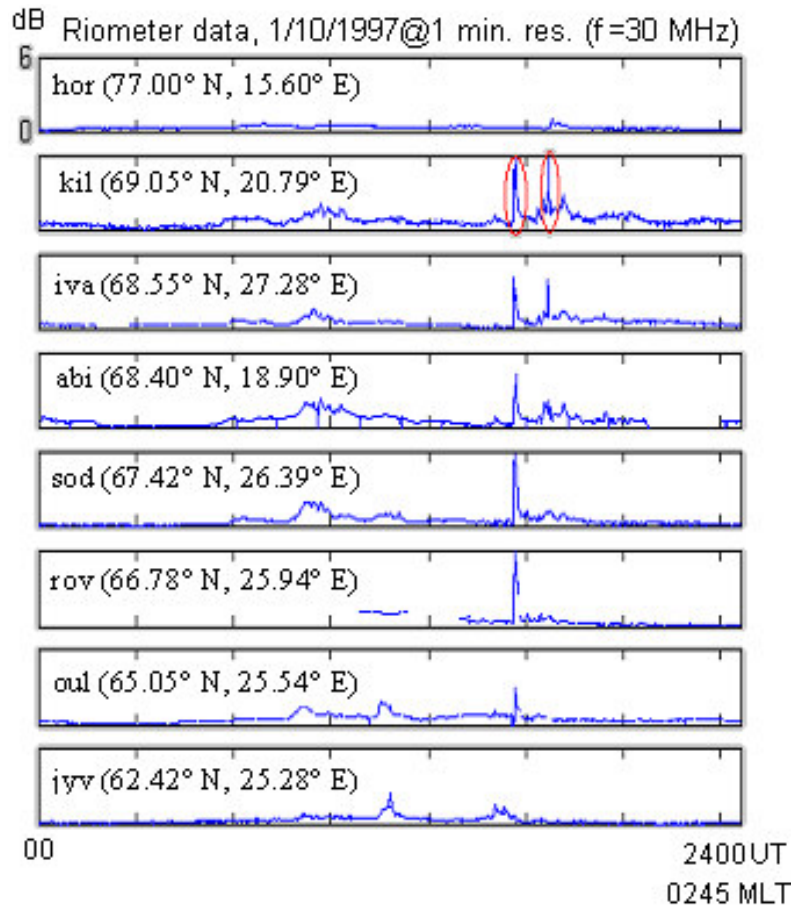


**Fig. 9.** Occurrence of spikes in SGO riometer chain for day 1 October 1997 00:00–24:00 UT (02:45 MLT) at 1-min resolution. Geographic latitude and longitude of stations are in brackets. The corrected geomagnetic (CGM) latitude of riometer stations at altitude of 90 km are given in Table 2. Data is scaled between 0 and 6 dB.

**Table 2.** Geographic coordinates and corrected geomagnetic (CGM) coordinates of riometer stations at altitude of 90 km for spike event Fig. 9.

Riometer Station	Geographic coordinates	Geomagnetic coordinates
Hornsund, Svalbard (hor)	77.00° N 15.60° E	74.03° N 110.49° E
Kilpisjärvi, Finland (kil)	69.05° N 20.79° E	65.83° N 104.41° E
Ivalo, Finland (iva)	68.55° N 27.28° E	64.99° N 109.09° E
Abisko, Sweden (abi)	68.40° N 18.90° E	65.28° N 102.42° E
Sodankylä, Finland (sod)	67.42° N 26.39° E	63.89° N 107.61° E
Rovaniemi, Finland (rov)	66.78° N 25.94° E	63.26° N 106.84° E
Oulu, Finland (oul)	65.05° N 25.54° E	61.51° N 105.49° E
Jyväskylä, Finland (jyv)	62.42° N 25.28° E	58.80° N 103.93° E

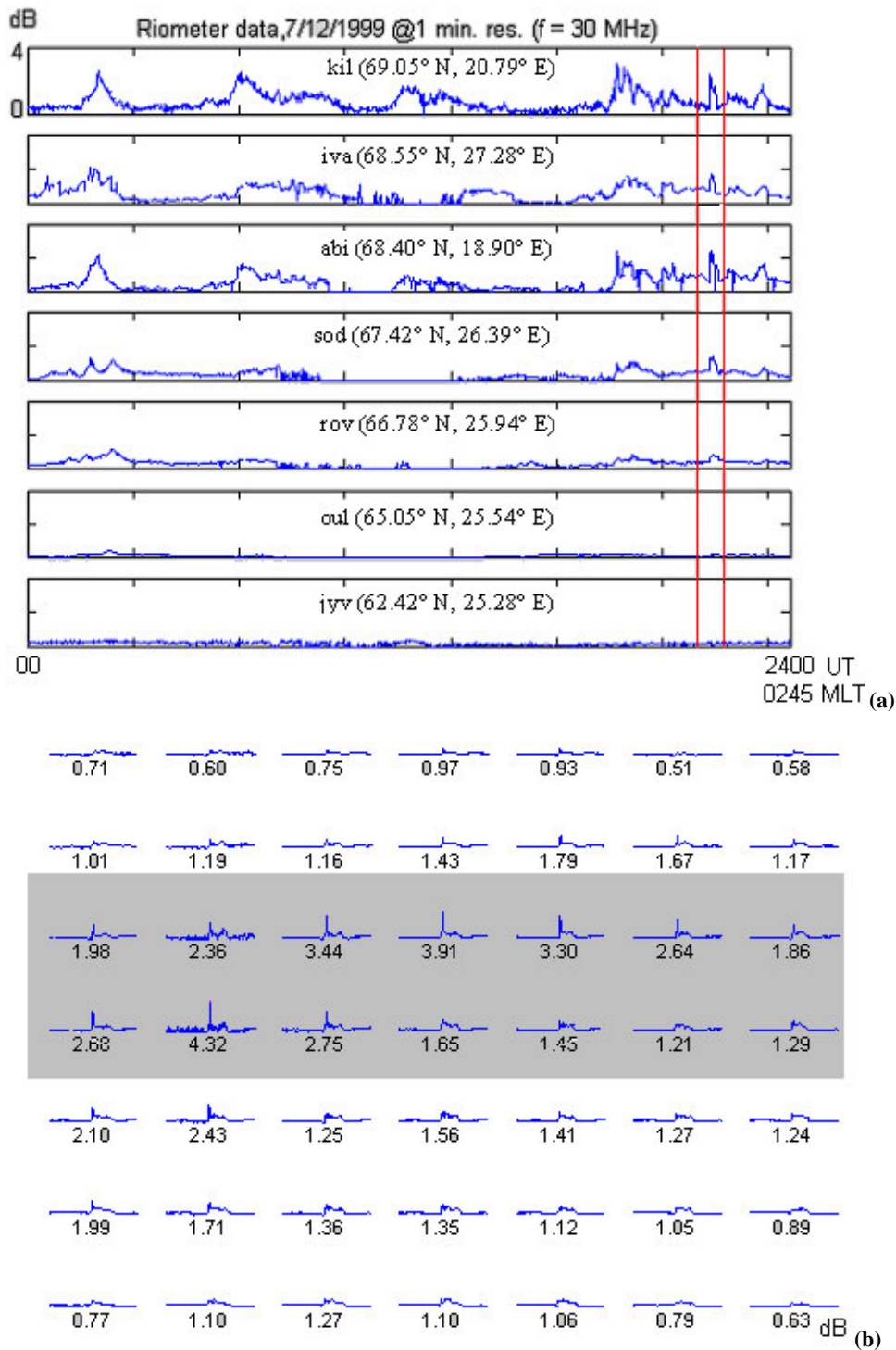


**Fig. 10.** (a) Occurrence of spikes in SGO riometer chain for day 7 December 1999 00:00–24:00 UT (02:45 MLT) at 1-min resolution. Geographic latitude and longitude of stations are mentioned in brackets. Data is scaled between 0 and 4 dB. Red lines highlight the spikes occurred between 21:00–22:00 UT (23:45–00:45 MLT). (b) IRIS field of view for event 7 December 1999 21:00–22:00 UT (23:45–00:45 MLT). Data are at 10-s resolution. Numbers are the peak of absorption in dB in each narrow-beam. Grey area highlights narrow-beams with the highest spikes.

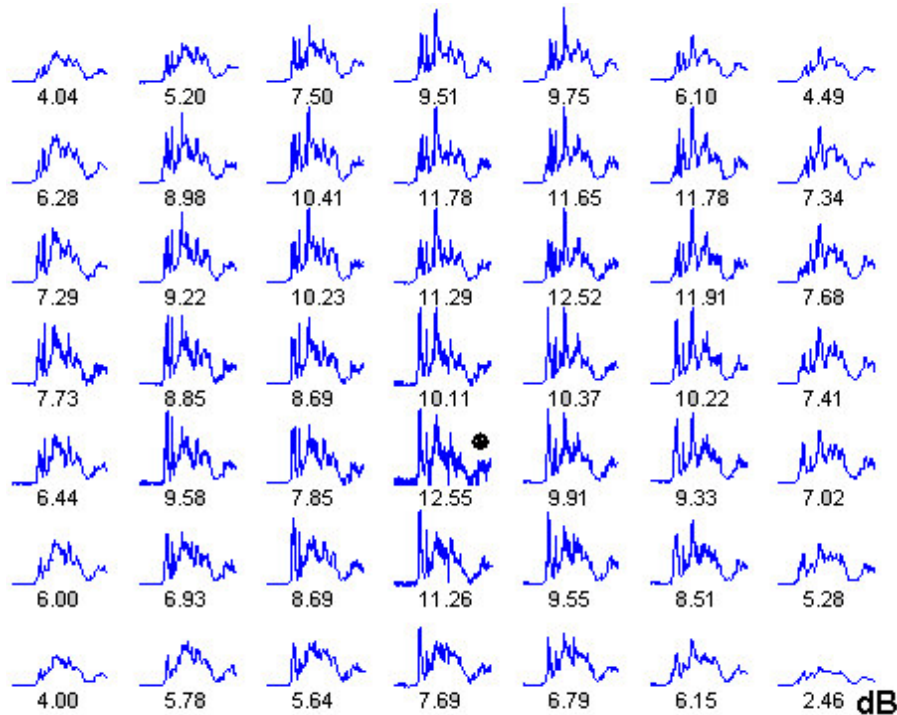


**Fig. 11.** A typical type IV spike event in IRIS FoV. Event occurred in 30 October 1994 19:30–20:30 UT (22:15–23:15 MLT). Numbers are the peaks of spikes in each narrow-beam in dB at 10-s resolution. Black spot in the middle marks the narrow-beam in which the most intense spike occurred.

corrected geomagnetic (CGM) latitude of riometer stations at altitude of 90 km are given in Table 2.

It is also useful to note that spikes that appear in the SGO chain often appear to be localised in the IRIS FoV. Figure 10 provides an example of this; the event is recorded by the SGO chain between latitudes of  $66.78^{\circ}$  N and  $69.05^{\circ}$  N and between longitudes of  $18.90^{\circ}$  E and  $27.28^{\circ}$  E. The rising time of spike event is the same for all stations but the peak of spike occurred slightly later in the lower latitudes (Fig. 10a). Although the main event is also seen in the most of IRIS FoV, the spike is only observed in a few narrow beams of IRIS (Fig. 10b).

Despite the similar appearance of the 4 types of spikes in the SGO chain their occurrence in the IRIS FoV was different. While the type IV spikes had the most coverage in the IRIS FoV, type I and type III spikes tend to be more limited and appeared in fewer narrow-beams. Statistically we measured the number of narrow-beams in which the intensity of spikes was more than 80% of the peak of each event.

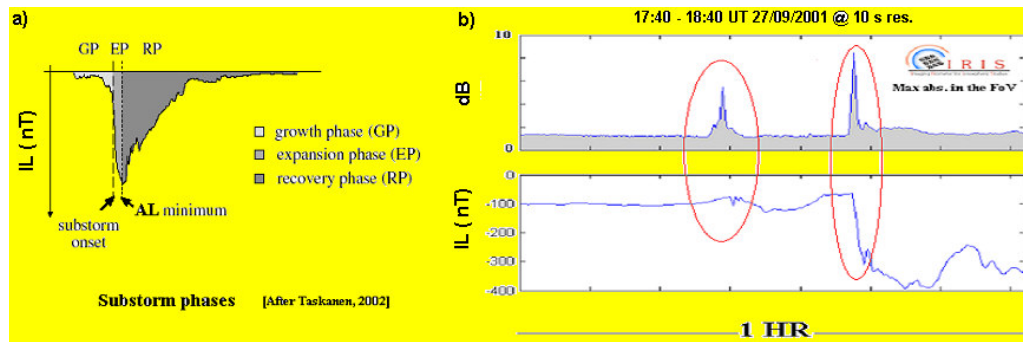
On average spikes appeared in more than 10 narrow-beams for type IV, 6 narrow-beams in type II and 5 and 3 narrow-beams in type I and III, respectively. The beamwidth of the narrow-beams varies between  $11.2^{\circ}$  and  $13.9^{\circ}$  and the distance between adjacent beam centres is approximately 31 km at 90-km altitude.

Figure 11 shows a typical type IV spike event in IRIS FoV in which a similar structure is observed in the most of narrow-beams.

### 3.7 Relation of spike events to the substorm development

In previous studies a strong link between absorption spikes and substorms has been identified. Hargreaves et al. (1997) encountered spikes as the ground-based signatures of substorms, which occur at or near the onsets. Substorms are comprised of 3 different phases which are distinguished by the variation of local AL index (Tanskanen, 2002); each event begins with a growth phase in which energy transfer from the solar wind to the magnetosphere is increased. The growth phase can be accompanied with the occurrence of pseudobreakups (e.g. McPherron, 1991). The most easily distinguishable phase of substorm is the expansion phase in which the substorm onset occurs. In this phase the energy, which has been already stored in the magnetotail during the growth phase, is released leading to a sudden increase in the westward electrojets. At the end of the expansion phase the AL index reaches a minimum, which is then followed by a recovery to near zero during the recovery phase of the substorm (Tanskanen, 2002).

Figure 12a illustrates 3 phases of an ideal substorm according to the variation in the IL index. During the growth



**Fig. 12.** (a) Phases of an ideal substorm is illustrated according to variation of IL index (After Taskanen, 2002). (b) Two spikes as signatures of pseudobreakup and substorm onset according to IL index variations. Event occurred in 27 September 2001 during 17:40–18:40 UT (20:25–21:25 MLT)

phase the IL index decreases slightly. The start of expansion phase is distinguished via the sharp slope of the decrease. However it is not always easy to determine the phases of substorms using the IL index due to the complicated nature of substorm development.

Besides, for consecutive substorms the growth phase of a new substorm is hard to identify from the signatures of extra intensifications during the recovery phase of the previous one (Taskanen, 2002).

Another issue arises when attempting to distinguish substorms from pseudobreakups since they have common features such as particle injections, magnetic Pi2 pulsations and aurora (Aikio et al., 1999). In the literature the signatures of pseudobreakups are identified from their low magnetic intensities (<100 nT) and short duration of less than 10 min (McPherron, 1991). Pseudobreakups may be isolated or occur during substorms.

In general absorption spikes are accompanied by a decrease in the IL index. During type I spikes the IL index decreases and recovers within a few minutes with the increase and decrease being of similar time-spans. For type II the recovery time is much longer (see Fig. 1a).

The variation of the IL index during type I was small such that in 60% of events the absolute variation of the IL index was less than 300 nT. Although this is stronger than 100 nT quoted by Pulkkinen (1996), type I spikes could be the absorption signature of pseudobreakups due to their short and sharp temporal structure accompanied by small absorption injections and a minimum variation in IL index as well as occurrence of Pi2 pulsations in magnetometer data around the onset of their peaks.

In at least 14% of events (12 out of 87 events) small type I spikes were observed shortly before more intense spikes. It is suggested that these small spikes are signatures of pseudobreakups during the growth phase of substorms as reported by McPherron (1991). Figure 12b gives an example of one such substorm with two successive spikes. The second spike

(type II) is associated with the substorm onset at the start of the expansion phase.

In 80% of type II spikes (130 out of 157 events) the peak of the spike is associated with the start of the expansion phase of a substorm as indicated by a sudden decrease in the IL index to values of minus a few hundred nT within a few minutes (Taskanen, 2002). The IL index reaches a local minimum and then recovers; this may take from hundreds of seconds to tens of minutes.

The recovery phase is longer (of the order of tens of minutes) for type II spikes. Pi2 pulsations in the IL index are observed in these events in the expansion phase. Similar pulsations are observed in the same time in the spikes and magnetic field components.

The dominant west/northward motion of type II spikes is consistent with the westward electrojet and poleward motion of auroral arc during substorms (Akasofu, 1977). The direction of spikes was reported as being mostly northward and westward for those occurring in the northern hemisphere (Hargreaves et al., 2001).

Figure 13 is an example of a type II spike. This event is the largest observed spike out of the 450 events, peaking at 14.85 dB at 10-s resolution. The spike rises from the noise level and peaks within a minute. It then decreases and is followed by injection absorption, which lasts for ~20 min. The absorption data and corresponding IL index during the growth phase are shown in the red ovals in Figs. 13a and 13b, respectively. The expansion phase began once the absorption started to increase; the largest peak of pulsation appeared at 18:48:10 UT (21:33:10 MLT) in the absorption data and one minute later Pi2 pulsations in the IL index peaked (21:34:10 MLT). The IL index reached minimum at 18:49:40 UT (21:34:40 MLT) and started to recover with the appearance of the injection absorption. The IL index varied between –200 and –256 nT during the growth phase then fell to –822 nT by the end of expansion phase (within 200 s) recovering to –350 nT by 19:30 UT (22:15 MLT), within one hour of the start of event.

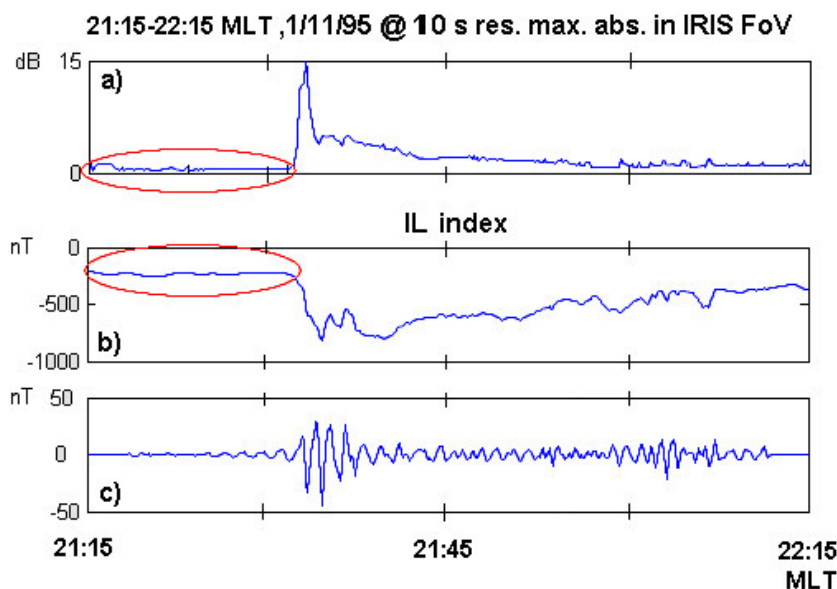


**Fig. 13.** (a) A typical example of type II spike event occurred in 1 November 1995 during 18:30–19:30 UT (21:15–22:15 MLT). (b) Variations of IL index during event (a). (c) Pi2 pulsations of IL index. Red ovals indicate the variations of absorption data and IL index during the growth phase of related substorm.

Similar to type I, type III spikes have short durations of a few minutes with small variations in the IL index such that in more than 50% of type III spikes the absolute variation of the IL index was less than 300 nT. However as opposed to type I, type III spikes are associated with injection absorption before the main spike. Pi2 pulsations in type III are observed after the injection and during the spikes both in the IL index and magnetic field components. The injection absorption before the spike in this type could be a signature of bursty bulk flows (BBF), appearing at the start of breakups or in the growth phase of substorms. BBFs are fast and narrow flows in near-Earth plasma sheet with azimuthal direction, lasting a few minutes and may happen during breakups and all 3 phases of substorms. They can appear as small-scale localised and/or large-scale global features (Grocott et al., 2004). Duration of type III spikes fit with the duration of BBFs and their few appearances in narrow beams of IRIS and the occurrences of similar spike events at lower latitudes at the same time indicate they can have a localised nature as well as more global responses. Possible connection between spike and BBF has also been mentioned in the previous study by Spanswick et al. (2005), however this speculation requires further investigation supported with magnetospheric data. Figure 1c shows a typical variation of the IL index during type III spike.

For type IV spike events the IL index displays a complicated variation. In 20% of events the peak of the absorption spike occurred after the minimum in the IL index, which means it occurred during the recovery phase of substorms.

Pi2 pulsations are observed in the magnetic field components whenever spikes occur and similar pulsations occurred more or less at the same time in the IL index. Type IV spikes are associated with the most intense substorms according to IL index variation and they are least localised within the IRIS FoV accompanied by observations of spikes in the SGO riometer chain. It is suggested that Type IV are signatures of multi-stage substorms, with more than one onset.

To compare the intensity and timing of spikes with those of corresponding magnetic activation, the peak and timing of the absorption spike was compared with the magnitude and timing of the minimum of the IL index for each event respectively; no linear dependence was found. Figure 14a shows the results of comparing the magnitudes of IL index for each type of spike; the most intense spikes, type I (mean of peak=5.1 dB) had the smallest magnitude of the IL index (mean = -325 nT, SD = 206). In the mean time the weakest spikes; type IV with the mean of peak of 3.9 dB had the most intense magnitude of IL index with a mean of -736 nT (SD=349 nT). For type II and III the mean of peak of spikes were 4.6 and 4.3 dB and the mean of minimum IL index were -553 (SD=265) and -354 nT (SD=196), respectively.

Figure 14b illustrates the results of the time delay between the occurrence of minimum IL index and peak of spikes for each type:

$$T_D = T_{\min IL} - T_s . \quad (2)$$

Where  $T_D$  is the delay time between minimum of IL and peaks of spikes,  $T_{\min IL}$  is the occurrence time of minimum of IL index and  $T_s$  is the occurrence time of peak of spike. For more than 75% of events the minimum of IL occurred

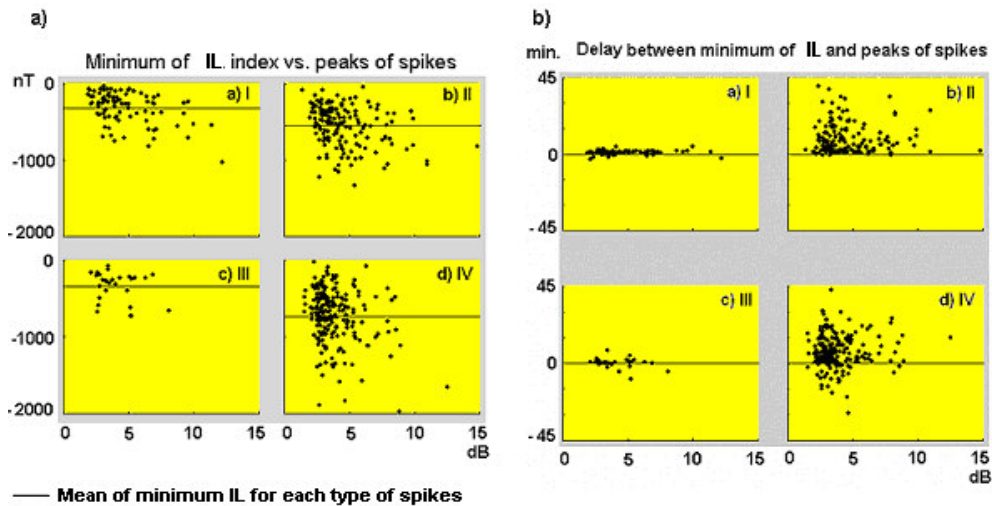


**Fig. 14.** (a) Scatter plot of minimum of IL index in nT versus peaks of spikes in dB for 4 types of spike events. Solid lines are the mean of minimum IL for each type. (b) Occurrence of time delay in minutes between minimum of IL index and peaks of spikes for 4 types of spike events (see Eq. 2).

within 15 min after the peak of the spike. The maximum of absolute time delay between the peak of the spike and minimum IL was only 4 min for type I, which is the shortest for all types. This time delay is consistent with the maximum 10-min duration of pseudobreakups suggested by McPherron (1991). In type II most of spikes peaked at or before the minimum of the IL index and for more than 80% of events the time delay was less than 15 min, which places them in the expansion phase of individual substorms. In 40% of type III spike events, the IL index reached its minimum before the peak of the spike. The maximum of absolute time delay between two parameters in type III was about 8 min. Type IV spikes had the maximum time delay; for more than 40% of events the absolute time delay was more than 15 min. In 20% of events the spike peaked after the minimum in the IL index within 15 min; therefore type IV spikes most likely appeared both in the expansion and recovery phases of substorms. Secondary spikes in the recovery phase can be considered as the signatures of successive substorms so type IV spikes seem to be indicators of multi-onset substorms.

#### 4 Summary and conclusion

Comprehensive study of absorption spike events based on large amount of data (450 events during years 1994–2003) and using multiple instruments (riometer data, magnetometer data and satellite X-ray images) has been performed.

This paper presents statistical studies of spike events and provides comparison with previous studies. For the first time analytical studies have been carried out for different classes of spikes providing insight into the nature and possible cause of spike events. Our statistical analysis of spike events illustrates:

- Distribution of occurrence of spike events is asymmetrical around MLM. Pre- midnight events are dominant so that 40% of spikes events occurred 1-2 hours before magnetic local midnight in IRIS FoV (centred at  $69.05^\circ$  N,  $20.79^\circ$  E,  $L \sim 6$ ). Results are consistent with previous study done on spike events by Taylor (1986) at Abisko ( $68.40^\circ$  N  $18.90^\circ$  E,  $L=5.81$ ) and occurrence of substorms (e.g. J.C. Gérard et al., 2004).
- Magnetic Pi2 pulsations are common feature of events. They were observed in components of magnetic field and in IL index when their variation is sharp and sudden, which is almost the same time that spikes have a peak. The highest cycle of damping sinusoidal pulsations was in the range of 10–14 mHz which is in the order of Pi2 pulsations of ULF frequencies in the inner magnetosphere (Keiling et. al., 2001).
- For those spike events in which PIXIE data were available, X-ray (2-12 keV) images of aurora was observed. It does confirm that high energetic particles mostly electrons with energy of a few keV to more than 30 keV are transferred from the magnetosphere to the ionosphere during spike events. Results are consistent with previous studies (e.g. Bjordal et al., 1971 and Pytte and Trefall, 1972).
- The occurrence (events per day) of spike events maximised during equinoxes and was minimum in summer (7 May–6 August); the results are consistent with the seasonal variation of occurrence of substorms (Hiebert et al., 2004).

- The mean intensity of spike events was maximum during autumn (7 August–5 November) and winter (6 November–4 February) and it was minimum during summer. This might be due to the fact that more energy is deposited by electron precipitation in the dark hemisphere than the sunlit hemisphere (Chua et al., 2004).
- Maximum occurrence (24%) and intensity (with mean of 5.1 dB) of spike events were observed in 1994–1995 that is the solar minimum activity. Year 2001, which was solar maximum, had the lowest occurrence (10%) of events as well as low intensity (mean of 4.0 dB) of events. Results are consistent with the occurrences of substorms (Heibert et al., 2004) and tend to be related to the high speed solar wind during solar minimum.
- More than 90% of spike events occurred in the periods of  $K_p > 3$  and spike events in the periods of low  $K_p$  index ( $K_p \leq 3$ ) only occurred after 17:00 UT (19:45 MLT). This is consistent with the results of study done by Nielsen (1980).
- Wavelet analysis of spike events in one-hour periods at 10-s resolution by Morlet wavelet has shown that most of the wavelet power spectrum lies in the frequencies up to 50 mHz, although for sharp spikes modulation in frequency can reach up to 300 mHz.

Previous work on spikes in a period of 5–10 min using the Morlet wavelet specified two important modulations between 16–67 mHz and 100–200 mHz (Hargreaves et al., 2001). We didn't observe any discontinuity of frequency modulations for those lasting up to 300 mHz. This might be due to the longer period of our data (1 h), which covers the injection absorption.

Classification of spikes have been performed by Spanwick et al. (2005) in connection with substorm onset and expansion phase, however, for the first time the temporal structure of spikes is linked with the variation of local electrojet data (IL index) to identify pseudobreakup and substorm development. Our study has identified four types of spikes with following description:

- Spikes without injection absorption (type I, Fig. 1a) had the shortest duration in time in order of few minutes.
- Spikes followed by injection absorption (type II, Fig. 1b) normally start with sharp increase in absorption intensity and decays in order of tens of minutes.
- Spikes of type III (Fig. 1c) occur after injection absorption with the duration of few minutes.
- Type IV spikes are embedded in injection absorption and have the longest duration in time in order of tens of minutes (Fig. 1d).

Statistical analysis have been performed on all these types of spikes in order to understand their relation with respect to the variation of IL index, MLT dependence, seasonal and yearly distribution, the direction of motion of spikes and their localisation. Maximum intensity in type I spikes was the highest with the mean of 5.1 dB. In 60% of spikes of type I absolute variation of IL index is less than 300 nT. They tend to be signatures of pseudobreakups according to the insignificant amount of injection absorption and short and small variation of IL index.

In 80% of type II spikes the peak of spikes is associated with the start of expansion phase of a substorm according to IL index variations. They can be considered as indicators of isolated substorms and their dominant west/northward motion in the IRIS FoV supports this assumption.

Type III spikes (27 out of 450) had the variation of IL index with mean of minimum –354 nT. They are the most localized type (determined from IRIS field of view). More events with supporting magnetospheric data are needed to associate type III spikes with any magnetospheric phenomenon/ substorm development.

The distribution of type IV spikes (45% of events) was shifted to the later hours of night as the peak was between 20:00–23:00 UT (22:45–01:45 MLT). They are the least localized of the four types. Their intensity in dB was minimum among all 4 types with the mean of 3.9 dB. In the mean time they were associated with the most intense variation of IL with the mean of minimum –736 nT. Time delay between minimum of IL index and peak of spikes was maximum in this type and their characteristics best fit with intense multi-onset substorms.

All classes of spike events have similar pattern in autumn and winter (Fig. 3b), however, type III spikes were not observed during summer and had the maximum of occurrence during spring (10%). Type II spikes maximum occurrence was found to be in summer (44%).

While years 1994 (solar minimum) and 1995 had the maximum occurrence for types I, II and III, minimum occurrence was in year 2001 (solar maximum) for type I and III. For type II and IV minimum occurrence was in the years 2002 and 2000, respectively.

The percentage of spikes events which occurred after MLM (between 21:00 and 24:00 UT) is different for each type. In type I spikes 32%, type II spikes 22%, type III spikes 22% and in type IV spikes 44% events occurred after local magnetic midnight. The highest occurrence of spike events is during 19:00–22:00 UT (21:45–00:45 MLT) with highest intensity between 2 and 12 dB.

Despite the similar appearance of 4 types of spikes in SGO chain of riometers, their appearance in the IRIS FoV was different. Type I and type III spikes tend to be more localized and appeared in few narrow-beams while type IV spikes had the most coverage of IRIS FoV.

In type I and type II spikes the number of west/northward events was more than east/southward events. No special

direction was dominant for type III and IV spikes. The mean of peak of spikes is slightly higher for west/north-ward spikes than east/south-ward spikes in all types of spikes.

We eliminated the early morning high absorption events (events occurred after 24:00 UT ~02:45 MLT) as we found their duration take more than 1-h and their intensities are lower than those of night-time spike events besides no specific relation between their occurrences and variations of magnetic components was observed.

Finally, based on seasonal variation of discrete aurora described by Hamrin et al. (2005) one may conclude that in the absence of sunlit ionosphere, density depletions lead to increased acceleration of energetic electrons consequently the source of spike events is the enhanced flux of electrons of a few to 10 s of keV as opposed to 100 s of keV. The next step is to find out the locations of source of different types of spikes to model each type of spikes based on its characteristics.

*Acknowledgements.* The data originated from the Imaging Riometer for Ionospheric Studies (IRIS), operated by the Department of Communications Systems at Lancaster University (UK) in collaboration with the Sodankyla Geophysical Observatory, and funded by the Particle Physics and Astronomy Research Council (PPARC). The authors thank the SAMNET team for magnetometer data. SAMNET is a PPARC National Facility operated by Lancaster University. We also thank the institutes who maintain the PIXIE images and IMAGE magnetometer array.

Topical Editor I. A. Daglis thanks two referees for their help in evaluating this paper.

## References

- Aggson, T. L., Heppner, J. P., and Maynard, N. C.: Observations of large magnetospheric electric fields during the onset phase of substorm, *J. Geophys. Res.*, 88, 3981–3990, 1983.
- Aikio, A. T., Sergeev, V. A., Shukhtina, M. A., Vagina, L. I., Angelopoulos, V., and Reeves, G. D.: Characteristics of pseudobreakups and substorms observed in the ionosphere, at the geosynchronous orbit, and in the mid-tail, *J. Geophys. Res.*, Vol.104, No.A6, 12 263–12 287, 1999.
- Akasofu, S.-I.: *Physics of Magnetospheric Substorms*, D. Reidel, Pub. Co., Dordrecht, Holland, 619, 1977.
- Baker D. N., Stauning, P., Hones, E. W., Higbie, P. R., and Belian, R. D.: Near equatorial high resolution measurements of electron precipitation at  $L \approx 6.6$ , *J. Geophys. Res.*, 86, 2295–2313, 1981.
- Baker, D. N., Pulkkinen, T. I., Angelopoulos, V., Baumjohann, W., and McPherron, R. L.: Neutral line model of substorms: Past results and present view. *J. Geophys. Res.*, 101, 12 975–13 010, 1996.
- Bjordal, J., Trefall, H., and Ullaland, S.: On the morphology of auroral-zone X-ray events – I Dynamics of midnight events, *J. Atmos. Terr. Phys.*, 33, 605–626, 1971.
- Chua, D., Parks, G., Brittacher, M., Germany, G., and Spann, J.: Auroral substorm timescales: IMF and seasonal variations, *J. Geophys. Res.*, 109, A03207, doi:10.1029/2003JA009951, 2004.
- Gérard, J. C., Hubert, B., Grard, A., Meurant, M., and Mende, S. B.: Solar wind control of auroral substorm onset locations observed with the IMAGE–FUV imagers, *J. Geophys. Res.*, 101, 109, A03208, doi:10.1029/2003JA010129, 2004.
- Grocott, A., Yeoman, T. K., Nakamura, R., Cowley, S. W. H., Frey, H. U., Rème, H., and Klecker, B.: Multi-instrument observations of the ionospheric counterpart of a bursty bulk flow in the near-Earth plasma sheet, *Ann. Geophys.*, 22, 1061–1075, 2004.
- Hamrin, M., Norqvist, P., Rönmark, K., and Fellgård, D.: The importance of solar illumination for discrete and diffuse aurora, *Ann. Geophys.*, 23, 3481–3486, 2005.
- Hargreaves, J. K., Browne, S., Ranta, H., Rosenberg, T. J. and Detrick, D. L.: A study of substorm-associated spike events in auroral absorption using imaging riometers at South Pole and Kilpisjärvi, *J. Atmos. Terr. Phys.*, 59, No.8, 853–872, 1997.
- Hargreaves, J. K., Chivers, H. J. A., and Nielsen, E.: Properties of spike events in auroral radio absorption, *J. Geophys. Res.*, Vol.84, No.A8, 4245–4250, 1979.
- Hargreaves, J. K., Ranta, A., Annan, J. D., and Hargreaves, J. C.: Temporal fine structure of night-time spike events in auroral radio absorption, studied by a wavelet method, *J. Geophys. Res.*, vol. 106, No. A11, 24 621–24 636, 2001.
- Hiebert, T., Donovan, E., and Jackel, B.: Substorm Seasonal and Solar Cycle Dependence (Poster), 7th International Conference on Substorms (ICS7), Finland, ICS7-A-00073, 2004.
- Holter, O., Perraut, S., Roux, A., Altman, C., Korth, A., Pecseli, H. L., Trulsen, J. and Pedersen, A.: Structure of low frequency oscillations at substorm breakup, in *Proceedings, Third International Conference on Substorms*, Versailles, France, Eur. Space Agency Spec. Publ., ESA SP-389, 393–398, 1996.
- Imhof, W. L., Spear, K. A., Hamilton, J. W., Higgings, B. R., Murphy, M. J., Pronko, J. G., Vondrak, R. R., McKenzie, D. L., Rice, C. J., Gorney, D. J., Roux, D. A., Williams, R. L., Stein, J., Bjordal, J., Stadsnes, J., Njüten, K., Rosenberg, T. J., Lutz, L., and Detrick, D.: The Polar Ionospheric X-ray Imaging Experiment (PIXIE), *Space Sci. Rev.*, 71, 385–408, 1995.
- Jacobs, J. A., Kato, Y., Matsushita, S., and Troitskaya, V. A.: Classification of geomagnetic micro pulsations, *J. Geophys. Res.*, 69, 180–181, 1964.
- Kavanagh, A. J., Kosch, M., Honary, F., Senior, A., Marple, S. R., Woodfield, E. E., and McCrea, I. W.: The statistical dependence of auroral absorption on geomagnetic and solar wind parameters, *Ann. Geophys.*, 22, 877–887, 2004.
- Keiling, A., Wygant, J. R., Cattell, C., Kim, K.-H., Russell, C. T., Milling, D. K., Temerin, M., Mozer, F. S., and Kletzing, C. A.: Pi2 pulsations observed with the Polar satellite and ground stations: Coupling of trapped and propagating fast mode waves to a midlatitude field line resonance, *J. Geophys. Res.*, 106, 25 891–25 904, 2001.
- Kennel, C. and Petschek, H. E.: Limit on stably trapped particle fluxed, *J. Geophys. Res.*, 71, 1–28, 1966.
- McPherron, R. L.: Physical processes producing magnetospheric substorms and magnetic storms, in: *Geomagnetism*, edited by: Jacobs, J. A., Academic, San Diego, USA., vol.4, 593–739, 1991.
- Nielsen, E.: Dynamics and spatial scale of auroral absorption spikes associated with the substorm expansion phase, *J. Geophys. Res.*, vol.85, No.A5, 2092–2098, 1980.
- Nielsen, E. and Axford, W. I.: Small scale auroral absorption events associated with substorms, *Nature*, 267, 502–504, 1977.
- Parthasarathy, R. and Berkey, F. T.: Auroral zone studies of sudden

- onset radio wave absorption events using multiple station and multiple frequency data, *J. Geophys. Res.*, 70, 89–98, 1965.
- Pulkkinen, T. I.: Pseudobreakup or substorm?, *Proc. Third International Conference on Substorms*, ESA-SP 389, 285–293, 1996.
- Pytte, T. and Trefall, H.: Auroral-zone electron precipitation events observed before and at the onset of negative magnetic bays, *J. Atmos. Terr. Phys.* 34, 315–337, 1972.
- Saito, T., Yumoto, K., and Koyama, Y.: Magnetic pulsation Pi2 as a sensitive indicator of magnetospheric substorm, *Planet Space Sci.*, 24, 1025–1029, 1976.
- Spanswick E., Donovan, E., Liu, W., Wallis, D., Aasnes, A., Hiebert, T., Jackel, B., Henderson, M., and Frey, H.: Substorm associated spikes in high energy particle precipitation, in: *The Inner Magnetosphere: Physics and modelling*, American Geophysical Union, USA, vol. 155, 227–236, 2005.
- Stauning, P. and Rosenberg, T. J.: High-latitude absorption spike events, *J. Geophys. Res.*, Vol.101, No.A2, 2377–2396,1996.
- Taylor, C. M.: A catalogue of spike events observed at Abisko, Sweden, 1 August 1979–31 July 1986, *Environmental Sciences Report TR/41*, Lancaster Univ., Dept. of Environmental Sciences, Lancaster, UK, 13, 1986.
- Tanskanen, E. I.: Terrestrial substorms as a part of global energy flow, PhD thesis, Department of Physical Sciences, University of Helsinki, Finland, 2002.
- Terkildsen, M. B., Fraser, B. J., Menk, F. W., and Morris, R. J.: Imaging riometer observations of absorption patches associated with magnetic impulse events, *S-RAMP Proceedings of the AIP Congress, ANARE*, Reports No. 146, 165–180, 2001.
- Torrence, C. and Compo G. P.: A practical guide to wavelet analysis, *Bulletin of the American Meteorological Society*: Vol. 79, No. 1, 61–78,1998.
- Yeoman, T. K. and Orr, D.: Phase and spectral power of mid-latitude Pi2 pulsations; Evidence for a plasmaspheric cavity resonance, *Planet. Space Sci.*, 37, 1367–1383, 1989.